ELSEVIER

Inorganica Chimica Acta 224 (1994) 81–95

Inorganica Chimica Acta

Phenylimido derivatives of $[Mo_6O_{19}]^{2-}$: syntheses, X-ray structures, vibrational, electrochemical, ^{95}Mo and ^{14}N NMR studies

Anna Proust*, René Thouvenot, Marc Chaussade, Francis Robert, Pierre Gouzerh*

Laboratoire de Chimie des Métaux de Transition, URA-CNRS No. 419, Case 42, Université Pierre et Marie Curie, 4 Place Jussieu, 75252 Paris Cedex 05, France

Received by Editor 24 January 1994; received by Publisher 17 May 1994

Abstract

Both $[Mo_6O_{18}(NPh)]^{2-}$ and $[Mo_6O_{17}(NPh)_2]^{2-}$ species are formed by reaction of $(n\text{-}Bu_4N)_2[Mo_6O_{19}]$ with either 1 or 2 equiv. of $Ph_3P{=}NPh$ in pyridine or acetonitrile and have been isolated as mixtures. Single-crystal X-ray diffraction analyses have shown that $[Mo_6O_{18}(NPh)]^{2-}$, $[Mo_6O_{17}(NPh)_2]^{2-}$ and $[Mo_6O_{19}]^{2-}$ can be found together in the same crystal of average composition $(n\text{-}Bu_4N)_2[Mo_6O_{19-x}(NPh)_x]$. The structural parameters of the averaged anions have been determined for $x=1.16$ (sample **1**) and $x=0.92$ (sample **2**). Crystal data for **1**: $a=12.684(4)$, $b=22.750(4)$, $c=19.483(3)$ Å, $\beta=103.04(2)°$, space group $P2_1/c$, $Z=4$, $R=0.048$ and $R_w=0.051$ for 3846 reflections with $I\geqslant 3\sigma(I)$. Crystal data for **2**: $a=12.678(2)$, $b=22.645(3)$, $c=19.462(4)$ Å, $\beta=104.16(2)°$, space group $P2_1/c$, $Z=4$, $R=0.058$ and $R_w=0.061$ for 5243 reflections with $I\geqslant 3\sigma(I)$. The products have been studied in acetonitrile solution by ^{95}Mo and ^{14}N NMR spectroscopy, Raman spectrophotometry and electrochemistry. Each of these techniques has confirmed the presence of the mono- and bis-imido derivatives together with the parent species, and has allowed both the characteristics of the individual components and the composition of the solution to be determined; the results obtained by the different methods are in reasonable agreement.

Keywords: Crystal structures; ^{95}Mo NMR spectroscopy; ^{14}N NMR spectroscopy; Imido complexes; Polyoxomolybdate complexes; Molybdenum complexes

1. Introduction

The functionalization of polyoxometalates, i.e. the replacement of terminal oxo ligands by some other groups, is of current interest as (i) it might provide molecular models for selective oxidation and ammoxidation of olefins by heterogeneous catalysis and (ii) it results in a modification of the electronic structure and, eventually, of the molecular structure of the starting cluster. Imido [1,2], hydrazido [2], nitrido [2], diazenido [3], nitrosyl [4] and cyclopentadienyl [5] derivatives of $[Mo_6O_{19}]^{2-}$ have been reported and characterized by X-ray crystallography with the exception of the nitrido derivative [2]. Only one difunctionalized Lindqvist-type compound, namely $[W_6O_{17}(Cp^*)_2]$ [6] has been characterized to date. Synthetic routes to derivatized Lindqvist-type hexametalates involve (i) reactions of hydrazido or imido mononuclear complexes with polyoxomolybdates [2], (ii) reactions of polyoxomolybdates with monosubstituted organohydrazines [3], hydroxylamine [4] or phosphinimines [1], and (iii) controlled oxidation of $[Cp^*M(CO)_2]_2$ [5,6]. With the possible exception of the tolylimido [1] and phenyldiazenido [3a] derivatives, these reactions do not proceed through direct substitution of $[Mo_6O_{19}]^{2-}$, which is not surprising since the latter is known to be quite non-basic [7] and unreactive. The functionalization of $[Mo_6O_{19}]^{2-}$ may result in its activation: indeed, $[Mo_6O_{18}(NO)]^{3-}$ reacts with dimethylsulfate to yield $[Mo_6O_{17}(OMe)(NO)]^{2-}$ in conditions where $[Mo_6O_{19}]^{2-}$ is not reactive. This activation has been primarily ascribed to the increase in charge density on the surface oxygen atoms as a tetravalent $[MoO]^{4+}$ unit is replaced by a trivalent $[Mo^{II}(NO)]^{3+}$ unit [4b].

*Corresponding authors.

SSDI 0020-1693(94)04110-H

We have been interested for some time in organoimido derivatives of polyoxometalates. The reaction of $(n\text{-}Bu_4N)_2[Mo_4O_{10}(OMe)_4Cl_2]$ [8,9] with an excess of $Ph_3P{=}NPh$ in dry toluene was found to proceed slowly, yielding triphenylphosphine oxide and a dark red compound, which was assumed to be $(n\text{-}Bu_4N)_2[Mo_6O_{18}(NPh)]$ on the basis of its IR spectrum. Unfortunately, this compound could not be characterized by X-ray diffraction due to the poor quality of the crystals. Actually, it could be a mixture of mono- and poly-phenylimido derivatives of $[Mo_6O_{19}]^{2-}$ (vide infra). Later on, the apparent activation of $[Mo_6O_{18}(NO)]^{3-}$ towards electrophiles in comparison with $[Mo_6O_{19}]^{2-}$ led us to expect that the nitrosyl derivative should react more easily with phosphinimines. However, the recent results reported by Maatta and co-workers [1] prompted us to reinvestigate first the reactivity of $[Mo_6O_{19}]^{2-}$ towards $Ph_3P{=}NPh$. We report here the results of our studies.

2. Experimental

2.1. Materials

The following chemicals were purchased from Aldrich and used without further purification: sodium molybdate dihydrate, sodium tetrafluoroborate, tetra-n-butylammonium hydrogenosulfate, tetra-n-butylammonium bromide, *N*-(triphenylphosphoranylidene)aniline, anhydrous pyridine, HPLC-grade acetonitrile. Reagent-grade acetonitrile was dried over calcium hydride and stored under a nitrogen atmosphere over activated 3 Å molecular sieves. Tetra-n-butylammonium tetrafluoroborate was synthesized from $n\text{-}Bu_4NHSO_4$ and $NaBF_4$ and dried overnight at 80 °C under vacuum. $(n\text{-}Bu_4N)_2[Mo_6O_{19}]$ was prepared as described in the literature and recrystallized from acetone [10]. Elemental analyses were performed by the Service Central d'Analyse of the CNRS (Vernaison, France).

2.2. Reaction of $(n\text{-}Bu_4N)_2[Mo_6O_{19}]$ with $Ph_3P{=}NPh$

A mixture of $(n\text{-}Bu_4N)_2[Mo_6O_{19}]$ (3.50 g, 2.5 mmol) and $Ph_3P{=}NPh$ (1.765 g, 5.0 mmol) in anhydrous pyridine (20 ml) was stirred for 48 h at 85 °C under nitrogen. Addition of benzene (80 ml) to the orange–red solution led to the formation of an oil, which was redissolved in 20 ml of acetonitrile after separation from the supernatant solution. Addition of ether (80 ml) to the CH_3CN solution gave back an orange oil, which crystallized within a few minutes. This crude product was redissolved in 20 ml of acetone and diethyl ether (40 ml) was carefully layered on the solution. Orange crystals (**1**) formed after the solution was allowed to stand for a few hours. IR (cm^{-1}, KBr pellet): 3060(w) ν(C–H), 1580(w), 1330(w), 975(m) ν(MO=N), 955(vs) ν_{as}(Mo=O), 795(vs) ν_{as}(Mo–O–Mo). ^{95}Mo NMR (ppm, in CH_3CN/CD_3COCD_3 90/10, 297 K): 163, 146, 123, 81, 72, 65. ^{14}N NMR (ppm, in CH_3CN/CD_3COCD_3 90/10, 297 K): 33, 31.

A similar workup on the solution obtained by using 1 equiv. of $Ph_3P{=}NPh$ (0.882 g, 2.5 mmol) led to the isolation of another sample (**2**). *Anal.* Calc. for $(n\text{-}Bu_4N)_2[Mo_6O_{18}(NPh)]$: C, 31.70; H, 5.39; N, 2.92. Found: C, 31.54; H, 5.34; N, 2.98%. IR (cm^{-1}, KBr pellet): 3060(w) ν(C–H), 1580(w), 1330(w), 975(m) ν(Mo=N), 950(vs) ν_{as}(Mo=O), 795(vs) ν_{as}(Mo–O–Mo). Raman (CH_3CN): 1004 ν_s(Mo=O), 986 ν_s(Mo=O), 975 ν(Mo=N), 956 ν_{as}(Mo=O), 284 ν_s(Mo–O_c), 256 ν_s(Mo–O_c). ^{95}Mo NMR (ppm, in CH_3CN/CD_3COCD_3 90/10, 343 K): 148, 125, 68(t). ^{14}N NMR (ppm, in CH_3CN/CD_3COCD_3 90/10, 333 K): 31, 30.

The reaction also works in acetonitrile. A mixture of $(n\text{-}Bu_4N)_2[Mo_6O_{19}]$ (3 g, 2.2 mmol) and $Ph_3P{=}NPh$ (1.55 g, 4.4 mmol) in dried acetonitrile (15 ml) was refluxed under nitrogen for 60 h. The brown–red solution was treated as described above and yielded 2.11 g of a crude product, which was recrystallized in a mixture of acetone and ether. Orange crystals of **3** were deposited within a few hours. *Anal.* Found: C, 31.85; H, 5.32; N, 2.85%. IR (cm^{-1}, KBr pellet): 3060(w) ν(C–H), 1580(w), 1330(w), 975(m) ν(Mo=N), 950(vs) ν_{as}(Mo=O), 795(vs) ν_{as}(Mo–O–Mo). Raman (CH_3CN): 1004 ν_s(Mo=O), 985 ν_s(Mo=O), 975 ν(Mo=N), 956 ν_{as}(Mo=O), 285 ν_s(Mo–O_c), 257 ν_s(Mo–O_c), 242 ν_s(Mo–O_c). ^{95}Mo NMR (ppm, in CH_3CN/CD_3COCD_3 90/10, 343 K): 166, 148, 126, 78(t), 68(t). ^{14}N NMR (ppm, in CH_3CN/CD_3COCD_3 90/10, 343 K): 31, 30.

2.3. NMR studies

The ^{95}Mo NMR spectra were registered at 32.6 MHz (11.8 T) on an AM 500 Bruker spectrometer operating in the Fourier mode. About 2 ml of a ~0.05 M solution in acetonitrile were mixed with 0.22 ml d_6-acetone for field-frequency lock and put in a conventional 10 mm o.d. NMR tube. Variable temperature measurements were made using the internal Bruker BVT-1000 temperature control unit driven by a copper-constantan thermocouple. The spectra were obtained using the commercial broad-band Bruker VSP probehead and were registered using the simple 'one pulse' excitation (10 μs, about 20° flip angle). Chemical shifts are given according to the IUPAC convention, with respect to an external 2 M aqueous alkaline Na_2MoO_4 solution. The ^{95}Mo NMR spectrum of sample **3** is shown in Fig. 1. ^{95}Mo NMR data are collected in Table 1.

The ^{14}N NMR spectra were registered in the same conditions at 36.1 MHz; the chemical shifts were obtained relative to acetonitrile acting as an internal reference and were recalculated with respect to neat

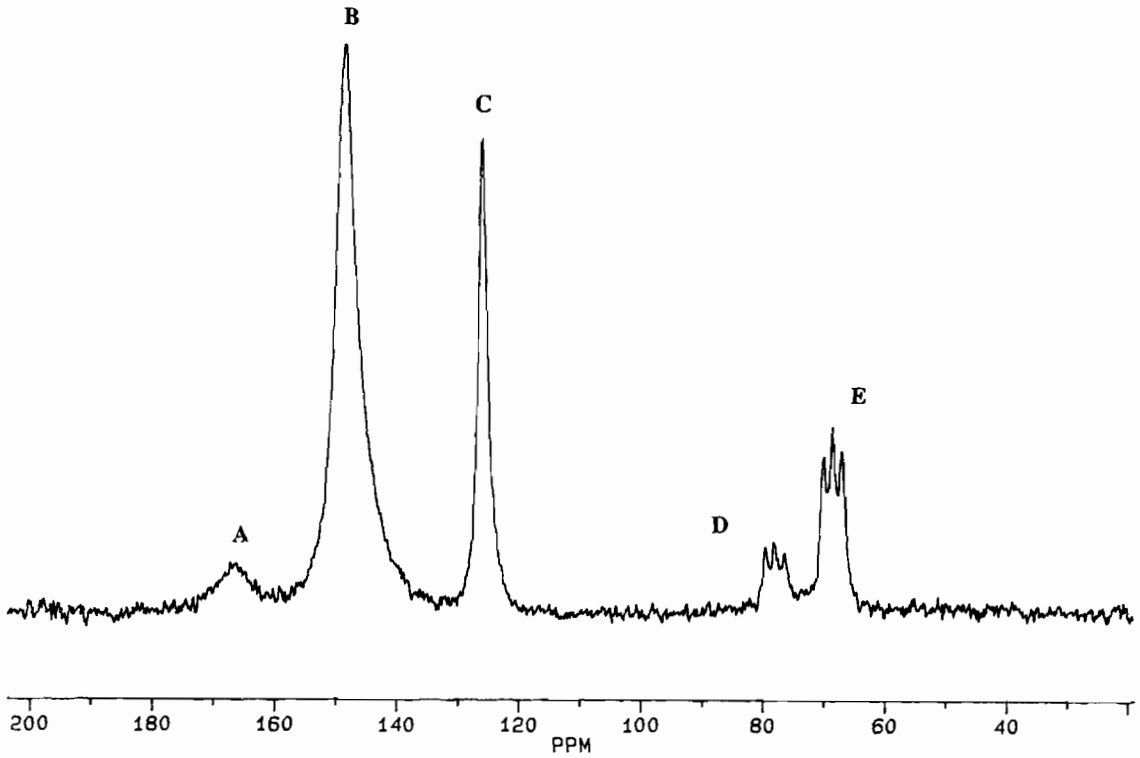

Fig. 1. 32.6 MHz ^{95}Mo NMR spectrum of sample **3** in acetonitrile/d_6-acetone solution. Experimental conditions: concentration ~0.05 M, 343 K, spectral width 6000 Hz (184 ppm), 32 000 transients, pulse width 10 μs (~20° flip angle), acquisition time 0.17 s, without recycle delay, line broadening 5 Hz.

Table 1
^{95}Mo NMR data[a,b]

Anion	*Mo*=O			*Mo*=N				δ_{wt}[c]
	δ	$\Delta\nu_{1/2}$[d]	n_{Mo}	δ	$\Delta\nu_{1/2}$[d]	n_{Mo}	^1J(Mo–N)[e]	
$[Mo_6O_{19}]^{2-}$	125	50	6					125
$[Mo_6O_{18}(NPh)]^{2-}$	148	125	4	68	30	1	49	131
	125[f]		1					
$[Mo_6O_{17}(NPh)_2]^{2-}$	166	125	2	78	30	2	50	131
	148[f]		2					

[a]Spectra recorded at 343 K in acetonitrile/d_6-acetone solution.
[b]δ, chemical shifts in ppm with respect to an external solution of Na_2MoO_4 in alkaline D_2O.
[c]$\delta_{wt} = \frac{1}{6}\Sigma(\delta \times n_{Mo})$.
[d]Line width at half height, in Hz.
[e]Coupling constant in Hz (±1 Hz).
[f]See text.

liquid nitromethane ($\delta(CH_3CN/CH_3NO_2) = -135.83$ ppm [11]).

2.4. Vibrational studies

IR spectra were recorded from KBr pellets with a Nicolet model 550 spectrometer. Raman spectra were obtained in the conventional 90° configuration on the solutions used in NMR studies by means of a double-monochromator Jobin-Yvon U1000 spectrophotometer equipped with a Coherent Ar^+ laser and a photon-counting detector. The effective power of the 514.5 nm exciting line was between 200 and 500 mW and the slit apertures were fixed to 500 μm (spectral width about 5 cm^{-1}). For each sample, a survey spectrum was scanned in the range 50–1100 cm^{-1} with an increment of 1 cm^{-1}; then in the low-frequency (200–300 cm^{-1}) and the high-frequency (900–1050 cm^{-1}) regions, a scanning increment of 0.2 cm^{-1} was chosen to increase the accuracy of the frequencies. Raman data are given in Table 2. The low frequency part of the Raman spectrum of sample **3** is presented in Fig. 2.

Table 2
Selected Raman data[a,b]

Anion	ν(Mo=O)		ν(Mo=N)	'ν_s(MoO_c)'
	ν_s	ν_{as}		
$[Mo_6O_{19}]^{2-}$	986 (A_{1g})	956 (E_g)		285 (A_{1g})
$[Mo_6O_{18}(NPh)]^{2-}$	1004 (A_1)	956 (E)	975 (A_1)	256 (A_1)
$[Mo_6O_{17}(NPh)_2]^{2-}$				240 (A_1)

[a]Spectra recorded in acetonitrile/d_6-acetone solution.
[b]Wavenumbers in cm^{-1} ($\pm$ 1 cm^{-1}).

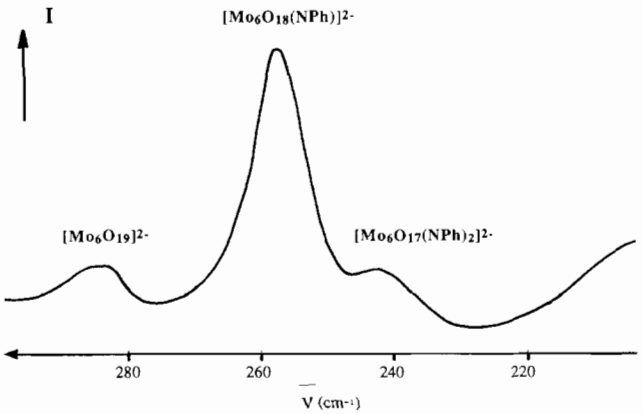

Fig. 2. Low wavenumber part of the Raman spectrum of sample **3** in acetonitrile solution.

2.5. Electrochemical studies

Electrochemical data were obtained in CH_3CN. Solutions were 0.1 M for the supporting electrolyte, n-Bu_4NBF_4, and $\sim 10^{-3}$ M for the sample under study; those of samples **2** and **3** were obtained by dilution of the solution used in NMR studies. Standard polarography at a dropping mercury electrode (DME) and polarography at a rotating platinum electrode were carried out on a Tacussel model PRG_3 device. Cyclic voltammetry (CV) at a platinum electrode was carried out on a PAR model 273 instrument. In any case, a standard three-electrode cell was used, which consisted of the working electrode, an auxiliary platinum electrode and an aqueous saturated calomel electrode (SCE) equipped with a double junction. A cyclic voltammogram of sample **1** is displayed in Fig. 3. Electrochemical data are given in Table 3; all potentials are relative to SCE.

2.6. Electronic spectroscopy

Electronic absorption spectra were recorded with a Shimadzu model UV-2101 spectrophotometer.

2.7. X-ray crystallographic studies

X-ray data were collected at room temperature with an Enraf-Nonius CAD4 diffractometer using graphite-monochromated Mo Kα radiation. Crystals were mounted on glass fibers. Lattice parameters and the orientation matrix were obtained from a least-squares fit of the setting angles of 25 automatically centered reflections. Data processing was performed on a MicroVAX II using the CRYSTALS system [12]. Intensities were corrected for Lorentz and polarization effects. Only the reflections with $I \geqslant 3\sigma(I)$ were kept in further calculations. The structures were solved with the use of direct methods (SHELXS 86 [13]). While the positions of all atoms of the hexamctalate framework and those of the carbon atoms of the tetrabutylammonium cations clearly showed up from Fourier maps, some difficulty arose in the location of the phenyl rings of the imido ligands. Indeed, in both **1** and **2**, difference Fourier maps revealed two substitution sites, A and B, which are mutually *cis*, with B being close to an inversion center. It was thought for some time that **1**, which was first studied by X-ray diffraction, was actually an equimolar mixture of $(n\text{-}Bu_4N)_2[Mo_6O_{18}(NPh)]$ and $(n\text{-}Bu_4N)_2[cis\text{-}Mo_6O_{17}(NPh)_2]$. Thus, the carbon atoms of rings A and B were assigned occupancy factors of 1.0 and 0.5, respectively. However, refinement of this statistical disordered model led to large equivalent isotropic thermal parameters for both rings A and B (up to 0.38 Å^2 for B). The situation is even more complicated in **2** since an inspection of the packing reveals that the presence of ring B in the anion (i) not only excludes that of ring B in the anion (ii) but also that of ring A in the anion (iii) (see Figs. 6 and 7). At this stage, results from NMR, Raman and electrochemical studies were available and it appeared that compounds **1** and **2** could contain $[Mo_6O_{19}]^{2-}$ as well as the mono- and bis-imido derivatives with a mean degree of substitution around 1. Then the carbon atoms of the phenyl rings were arbitrarily assigned adjustable isotropic thermal parameters (starting value; 0.12 Å^2) and occupancy factors (starting value: 0.5). Refinement of this model converged to U_{iso} values of 0.13 and 0.15 Å^2 and to site populations of 0.76 and 0.40 for rings A and B, respectively, for sample **1**. The corresponding values for sample **2** were 0.14 Å^2, 0.18 Å^2, 0.58 and 0.34. The degree of substitution, x, i.e. the number of phenylimido ligands per hexametalate anion reaches 1.16 in **1** and 0.92 in **2**. These values are consistent with those of $\sim$1.0 and 0.83, respectively, deduced from electrochemical and NMR data (see Table 8).

These site populations were kept fixed in further cycles of refinements and phenyl rings B were refined as rigid groups. Hydrogen atoms were not located nor were they introduced in idealized positions. Two distances, C(51)–C(52) and C(52)–C(53), within a tetrabutylammonium cation in **1** were constrained to 1.54 Å. An empirical absorption correction was applied using DIFABS [14]. Neutral-atom scattering factors were

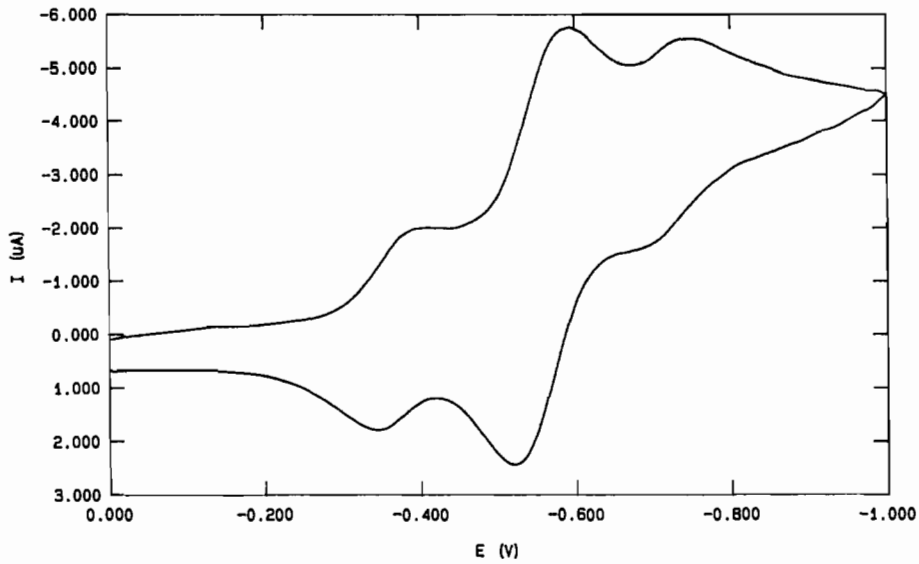

Fig. 3. Cyclic voltammogram of sample **1** in acetonitrile solution at a platinum electrode; 0.1 M in n-Bu_4NBF_4; scan rate 0.1 V s^{-1}; *E* vs. SCE.

Table 3
Electrochemical data[a,b] in CH_3CN[c]

Compound	$E_{1/2}$ (DME)	$E_{1/2}$ (Pt)	[m]/[h]	[m]/[b]	Ep_a (Pt)	Ep_c (Pt)	$1/2(Ep_a+Ep_c)$	(Ep_a-Ep_c)
$[Mo_6O_{19}]^{2-}$[d]		−0.37						
1 (recrystallized)		−0.36			−0.34	−0.39	−0.37	0.05
		−0.56	~3	~3	−0.52	−0.59	−0.56	0.07
		−0.73			−0.69	−0.75	−0.72	0.06
2	−0.37	−0.37			−0.33	−0.41	−0.37	0.08
	−0.55	−0.56	~2		−0.51	−0.61	−0.56	0.10
	?*	~ −0.74*						
3	−0.37	−0.37			−0.34	−0.39	−0.37	0.05
	−0.56	−0.56	~6	~9	−0.51	−0.59	−0.55	0.08
	−0.72	?*						

An asterisk indicates ill-defined.
[a] *E*, V vs. SCE.
[b] h = $[Mo_6O_{19}]^{2-}$; m = $[Mo_6O_{18}(NPh)]^{2-}$; b = $[Mo_6O_{17}(NPh)_2]^{2-}$.
[c] 0.1 M n-Bu_4NBF_4.
[d] Tetrabutylammonium salt.

used, with anomalous dispersion correction applied [15]. Crystal data and refinement parameters are summarized in Table 4. Final atomic coordinates and temperature factors for compounds **1** and **2** are listed in Tables 5 and 6, respectively. Selected bond distances and angles are given in Table 7. Drawings [16] of $[Mo_6O_{18}(NPh)]^{2-}$ and $[Mo_6O_{17}(NPh)_2]^{2-}$ are shown in Figs. 4 and 5, respectively. Packings of **1** and **2** are shown in Figs. 6 and 7, respectively. The following numbering scheme has been used for both compounds: terminal oxygen or nitrogen atoms are labelled X_i (X = O or N), where *i* is equal to the number of the molybdenum atom; bridging oxygen atoms (O_b) are labelled O_{ij}, where *i* and *j* refer to the labels of the bridged molybdenum atoms; the central oxygen atom (O_c) is labelled O(10).

3. Results and discussion

In acetonitrile or pyridine, $Ph_3P{=}NPh$ reacts on $[Mo_6O_{19}]^{2-}$ to give at least two phenylimido complexes, $[Mo_6O_{18}(NPh)]^{2-}$ and $[Mo_6O_{17}(NPh)_2]^{2-}$, which have been obtained as tetrabutylammonium salts. Solution and solid state studies lead to the conclusion that both crude and recrystallized samples are mixtures of several components including $(n\text{-}Bu_4N)_2[Mo_6O_{19}]$,

Table 4
Crystal data, data collection and refinement parameters for $(n\text{-}Bu_4N)_2[Mo_6O_{17.84}(NPh)_{1.16}]$ (**1**), $(n\text{-}Bu_4N)_2[Mo_6O_{18.08}(NPh)_{0.92}]$ (**2**) and **3**

Compound	**1**	**2**	**3**
Formula	$C_{38.96}H_{77.80}N_{3.16}Mo_6O_{17.84}$	$C_{37.52}H_{76.60}N_{2.92}Mo_6O_{18.08}$	
Formula weight (g mol^{-1})	1451.70	1433.67	
System	monoclinic	monoclinic	monoclinic
Space group	$P2_1/c$	$P2_1/c$	$P2_1/c$
a (Å)	12.684(4)	12.678(2)	12.680(5)
b (Å)	22.750(4)	22.645(3)	22.702(4)
c (Å)	19.483(3)	19.462(4)	19.461(6)
α (°)	90.00	90.00	90.00
β (°)	103.04(2)	104.16(2)	103.49(3)
γ (°)	90.00	90.00	90.00
V (Å^3)	5476(22)	5417(23)	5447(35)
Z	4	4	
μ(Mo Kα) (cm^{-1})	13.65	13.79	
ρ_{calc} (g cm^{-3})	1.761	1.758	
2θ Range (°)	$3 \leqslant 2\theta \leqslant 50$	$2 \leqslant 2\theta \leqslant 50$	
Scan type	$\omega/2\theta$	$\omega/2\theta$	
Scan width (°)	$0.8 + 0.345\text{tg}\theta$	$0.8 + 0.345\text{tg}\theta$	
Scan speed (° min^{-1})	$1.7 \leqslant$ s.p. $\leqslant 20.1$	$1.8 \leqslant$ s.p. $\leqslant 20.1$	
Octants collected	$\pm 14, +23, +20$	$-15 + 14, +25, +23$	
No. reflections collected	9487	9913	
No. unique reflections	9199	9468	
No. reflections with $I \geqslant 3\sigma(I)$	3846	5243	
No. variables refined	560	560	
Goodness of fit, s	2.76	3.88	
Absorption correction, cor_{max}	1.27	1.34	
cor_{min}	0.71	0.67	
R[a]	0.048	0.058	
R_w[b] ($w=1$)	0.051	0.061	

[a] $R = \Sigma\|\|F_o\| - \|F_c\|\|/\Sigma\|F_o\|$.
[b] $R_w = [\Sigma w(F_o - F_c)^2/\Sigma w F_o^2]^{1/2}$.

$(n\text{-}Bu_4N)_2[Mo_6O_{18}(NPh)]$, $(n\text{-}Bu_4N)_2[Mo_6O_{17}(NPh)_2]$ and, possibly, $(n\text{-}Bu_4N)_2[Mo_6O_{16}(NPh)_3]$ (vide infra).

3.1. NMR studies

Three samples, crude **1** and recrystallized **2** and **3**, were studied by NMR spectroscopy. The ^{95}Mo NMR spectra of these three samples present the same pattern of lines; however, the relative intensities of these lines vary from one sample to one another, which indicates the presence of more than one molybdenum species, possibly $[Mo_6O_{19}]^{2-}$, $[Mo_6O_{18}(NPh)]^{2-}$ and $[Mo_6O_{17}(NPh)_2]^{2-}$. The spectrum for $[Mo_6O_{19}]^{2-}$, which has idealized O_h symmetry, is known to display a single signal at ~125 ppm [3b,4b]; those of $[Mo_6O_{18}(NPh)]^{2-}$, where the hexametalate core has approximate C_{4v} symmetry, and of *cis*-$[Mo_6O_{17}(NPh)_2]^{2-}$, with approximate C_{2v} symmetry, should display three lines with relative intensities 1:4:1 and 2:2:2, respectively.

Let us first consider the spectrum of sample **2**, where the mono-imido species was expected to be most dominant, since it was obtained from an equimolar mixture of $[Mo_6O_{19}]^{2-}$ and $Ph_3P{=}NPh$. This spectrum displays three main signals at 148 (B), 125 (C) and 68 (E) ppm, as well as two weaker signals at 166 (A) and 78 (D) ppm. The peak at 125 ppm can be unambiguously attributed to $[Mo_6O_{19}]^{2-}$. At 343 K all signals sharpen as the quadrupolar relaxation rates of both ^{95}Mo and ^{14}N nuclei are lowered, and signals D and E appear as 1:1:1 triplets due to scalar coupling $^1J(^{95}\text{Mo}{-}^{14}\text{N})$. Consequently, these lines must be assigned to *Mo*=NPh centers. Peaks B and E are in relative intensities close to 4:1, which supports the assignment of peak B to the four equatorial *Mo*=O of the $[Mo_6O_{18}(NPh)]^{2-}$ species. The line from the remote axial *Mo*=O, *trans* to the Mo=NPh unit, is likely to be superimposed on line C. In the same way, peaks D and A, in relative intensities 1:1, are assigned, respectively, to the equivalent *Mo*=NPh and to two equivalent *Mo*=O of the *cis*-bis-imido $[Mo_6O_{17}(NPh)_2]^{2-}$ species (approximate symmetry C_{2v}). Indeed, the relative intensities of these peaks are higher for samples **1** and **3**, which were obtained using an excess of $Ph_3P{=}NPh$ (Fig. 1). Line A likely arises from the *Mo*=O *cis* to both Mo=NPh units, while the line from the two other equivalent *Mo*=O, which lie *cis* to one Mo=NPh unit and *trans* to the other, is likely to be superimposed on line B. This is supported by the following considerations.

- In the mono-imido, the *Mo*=N resonance is shielded by 57 ppm with respect to $[Mo_6O_{19}]^{2-}$, which is consistent with the higher π-donor ability of imido ligands with respect to the oxo ligand. On the other hand, the

Table 5
Fractional atomic coordinates[a] and temperature factors[b] for $(n\text{-}Bu_4N)_2[Mo_6O_{17.84}(NPh)_{1.16}]$ (**1**)

Atom	*x/a*	*y/b*	*z/c*	U_{eq}	U_{iso}
Mo(1)	0.1794(1)	0.14205(7)	−0.31979(8)	0.0755	
Mo(2)	0.4027(1)	0.15855(6)	−0.20092(7)	0.0686	
Mo(3)	0.2466(1)	0.04454(7)	−0.19755(8)	0.0785	
Mo(4)	0.4092(1)	0.12615(6)	−0.36484(7)	0.0626	
Mo(5)	0.2518(1)	0.01234(7)	−0.35982(8)	0.0777	
Mo(6)	0.4784(1)	0.02718(6)	−0.24000(7)	0.0713	
O(2)	0.4603(9)	0.2097(5)	−0.1436(6)	0.0917	
O(4)	0.4697(8)	0.1562(4)	−0.4247(5)	0.0815	
O(5)	0.198(1)	−0.0397(5)	−0.4181(6)	0.1115	
O(6)	0.5875(9)	−0.0140(5)	−0.2143(6)	0.1016	
O(10)	0.3244(6)	0.0850(4)	−0.2797(4)	0.0514	
O(12)	0.2712(8)	0.1908(4)	−0.2468(5)	0.0765	
O(13)	0.1391(7)	0.1004(5)	−0.2438(5)	0.0847	
O(14)	0.2760(7)	0.1664(4)	−0.3789(5)	0.0737	
O(15)	0.1440(8)	0.0739(5)	−0.3769(5)	0.0827	
O(23)	0.3273(8)	0.1093(4)	−0.1481(5)	0.0761	
O(24)	0.4564(7)	0.1761(4)	−0.2834(5)	0.0643	
O(26)	0.5105(7)	0.0962(4)	−0.1867(5)	0.0745	
O(35)	0.2001(8)	−0.0064(5)	−0.2789(5)	0.0888	
O(36)	0.3834(8)	0.0037(4)	−0.1821(5)	0.0748	
O(45)	0.3311(7)	0.0603(4)	−0.4125(4)	0.0714	
O(46)	0.5122(7)	0.0706(4)	−0.3177(5)	0.0688	
O(56)	0.3846(9)	−0.0198(4)	−0.3135(5)	0.0734	
X(1)	0.0708(9)	0.1892(7)	−0.3474(7)	0.0860	
X(3)	0.186(1)	0.0145(6)	−0.1365(7)	0.0957	
C(1)*	0.017(2)	0.245(1)	−0.362(2)		0.128(4)
C(2)*	0.002(2)	0.275(1)	−0.428(1)		0.128(4)
C(3)*	−0.054(2)	0.331(1)	−0.438(1)		0.128(4)
C(4)*	−0.097(2)	0.353(1)	−0.390(2)		0.128(4)
C(5)*	−0.097(2)	0.327(1)	−0.327(2)		0.128(4)
C(6)*	−0.032(2)	0.270(1)	−0.310(1)		0.128(4)
C(7)**	0.104(3)	0.011(2)	−0.096(2)		0.147(9)
C(8)**	0.131(3)	0.038(1)	−0.031(2)		0.147(9)
C(9)**	0.065(4)	0.032(2)	0.017(2)		0.147(9)
C(10)**	−0.028(4)	−0.002(2)	−0.001(2)		0.147(9)
C(11)**	−0.056(3)	−0.030(2)	−0.066(2)		0.147(9)
C(12)**	0.011(4)	−0.023(2)	−0.114(2)		0.147(9)
N(32)	−0.2058(9)	0.0400(6)	−0.3716(6)	0.0743	
C(33)	−0.115(1)	−0.0059(7)	−0.3576(8)	0.0744	
C(34)	−0.098(1)	−0.0370(8)	−0.4235(9)	0.0876	
C(35)	−0.035(1)	−0.0954(9)	−0.397(1)	0.1021	
C(36)	−0.022(1)	−0.1317(8)	−0.457(1)	0.1079	
C(37)	−0.226(1)	0.0619(8)	−0.3004(8)	0.0935	
C(38)	−0.125(1)	0.0922(9)	−0.2536(9)	0.1001	
C(39)	−0.159(2)	0.110(1)	−0.184(1)	0.1379	
C(40)	−0.193(4)	0.158(1)	−0.182(2)	0.2036	
C(41)	−0.312(1)	0.0144(7)	−0.4143(8)	0.0731	
C(42)	−0.344(1)	−0.0447(7)	−0.3834(8)	0.0802	
C(43)	−0.456(1)	−0.0618(8)	−0.4282(8)	0.0805	
C(44)	−0.489(2)	−0.1210(8)	−0.402(1)	0.1052	
C(45)	−0.170(1)	0.0899(7)	−0.4139(8)	0.0753	
C(46)	−0.251(1)	0.1423(7)	−0.426(1)	0.0912	
C(47)	−0.224(2)	0.1815(8)	−0.483(1)	0.1071	
C(48)	−0.300(2)	0.2363(8)	−0.495(1)	0.1214	
N(49)	0.428(1)	0.3387(5)	−0.4049(7)	0.0782	
C(50)	0.352(1)	0.3640(7)	−0.3650(9)	0.0866	
C(51)	0.296(2)	0.3193(8)	−0.325(1)	0.1088	
C(52)	0.222(2)	0.360(1)	−0.292(1)	0.1421	
C(53)	0.191(4)	0.324(1)	−0.234(2)	0.3512	
C(54)	0.470(1)	0.3922(6)	−0.4406(8)	0.0787	

(*continued*)

Table 5 (*continued*)

Atom	*x/a*	*y/b*	*z/c*	U_{eq}	U_{iso}
C(55)	0.559(1)	0.3779(7)	−0.4768(8)	0.0860	
C(56)	0.594(1)	0.4363(8)	−0.5089(9)	0.0971	
C(57)	0.688(1)	0.428(1)	−0.5428(9)	0.1042	
C(58)	0.524(1)	0.3050(7)	−0.3555(9)	0.0892	
C(59)	0.587(2)	0.3438(8)	−0.296(1)	0.1064	
C(60)	0.666(2)	0.299(1)	−0.252(1)	0.1237	
C(61)	0.737(2)	0.332(1)	−0.192(1)	0.1570	
C(62)	0.374(1)	0.2929(7)	−0.4593(8)	0.0805	
C(63)	0.275(2)	0.3140(8)	−0.5104(9)	0.0970	
C(64)	0.231(2)	0.2607(9)	−0.560(1)	0.1184	
C(65)	0.119(2)	0.279(1)	−0.611(1)	0.1375	

X(1) = 0.76 N + 0.24 O.
X(3) = 0.40 N + 0.60 O.
* occ = 0.76.
**occ = 0.40.
[a]E.s.d.s in the least significant digits are given in parentheses.
[b]$U_{eq} = [U(11) \cdot U(22) \cdot U(33)]^{1/3}$.

four Mo atoms adjacent to the Mo=NPh unit are deshielded by 23 ppm only with respect to $[Mo_6O_{19}]^{2-}$. For the remote molybdenum atom, the shift is expected to be even smaller and the assumption that the resonance meets that of $[Mo_6O_{19}]^{2-}$ seems justified.

• In the bis-imido anion, all observed resonances are deshielded with respect to those of $[Mo_6O_{18}(NPh)]^{2-}$. If each Mo=NPh group is assumed to induce a high-frequency shift of ~23 ppm on the resonance of the adjacent Mo atoms, then the line for the two Mo atoms *cis* to both Mo=NPh groups is expected to be found at ~171 ppm, which is in reasonable agreement with the value observed for peak A. In these conditions, the line arising from the two other Mo atoms which are *cis* to only one Mo=NPh group, should be superimposed to that of the four equatorial Mo atoms of the mono-imido derivatives (peak B). Indeed, the integrated intensity of line B is greater than four times that of line E, and the excess is nearly equal to the integrated intensity of each line of the bis-imido anion.

• Under this assumption it is worth noticing that the weighted chemical shift of the six Mo atoms of the hexametalate framework remains nearly unchanged through the oxo-imido substitution, which is consistent with the conservation of the overall charge density. Then, the individual shifts are essentially induced by modifications of the diamagnetic part of the shielding due to local charge density modifications.

Although the Mo atom carrying an imido ligand is dissymmetrically coordinated to five oxygen atoms and one nitrogen atom, its resonance is remarkably narrow (30 Hz at 343 K), which allows the observation of the one-bond coupling constants ^1J(Mo–N) (Fig. 1); the line width is comparable to that of the symmetrically coordinated molybdenum atoms in $[Mo_6O_{19}]^{2-}$. On the contrary the lines for the *Mo*=O groups *cis* to Mo=N are about twice broader.

Let us recall that for quadrupolar nuclei with dominant quadrupolar relaxation, the line width reflects directly the charge dissymmetry around the resonant nucleus.

$$T_{2q}^{-1} = \pi\Delta\nu_{1/2} = \frac{3\pi^2}{10}\,\frac{(2I+3)}{I^2(2I-1)}\left[\frac{e^2q_{zz}Q}{h}\right]^2\left(1+\frac{1}{3}\eta^2\right)\tau_c$$

where q_{zz} and η are, respectively, the largest component and the asymmetry parameter of the electric field gradient (e.f.g.) tensor at the resonant nucleus, eQ is the nuclear quadrupole moment. The difference between *Mo*=N and *Mo*=O resonances indicates a significant increase of the e.f.g. at the Mo atoms *cis* to the Mo=N group(s) although the coordinated atoms remain unchanged: this likely corresponds to an increased distortion of the MoO_6 octahedron, which however cannot be ascertained from the X-ray structural data.

The ratio of the concentration of the mono-imido species to that of the bis-imido one can be easily inferred from the relative intensities of the two triplets E and D; the calculated values of 1.5, 12 and 6 for samples **1**, **2** and **3**, respectively, are in agreement with those obtained from ^{14}N NMR data. The determination of the ratio of the concentration of the mono-imido species to that of $[Mo_6O_{19}]^{2-}$ is less obvious. For samples **2** and **3**, the integrated intensity of peak C was corrected for the contribution of the remote Mo atom from the mono-imido anion, estimated from the intensity of line E. This led to the ratio of 3 and 10 for samples **2** and **3**, respectively. It follows that sample **2** would contain 71% of $(n\text{-}Bu_4N)_2[Mo_6O_{18}(NPh)]$, 23% of $(n\text{-}Bu_4N)_2[Mo_6O_{19}]$ and 6% of $(n\text{-}Bu_4N)_2[Mo_6O_{17}(NPh)_2]$ and thus could be formulated as an

Table 6
Fractional atomic coordinates[a] and temperature factors[b] for $(n\text{-}Bu_4N)_2[Mo_6O_{18.08}(NPh)_{0.92}]$ (2)

Atom	x/a	y/b	z/c	U_{eq}	U_{iso}
Mo(1)	0.1798(1)	0.14246(6)	−0.32265(7)	0.0761	
Mo(2)	0.4063(1)	0.16086(6)	−0.20232(6)	0.0696	
Mo(3)	0.2540(1)	0.04485(6)	−0.19812(7)	0.0779	
Mo(4)	0.4105(1)	0.12802(5)	−0.36629(6)	0.0630	
Mo(5)	0.2577(1)	0.01241(6)	−0.36083(7)	0.0774	
Mo(6)	0.4861(1)	0.03004(5)	−0.23988(7)	0.0716	
O(2)	0.4641(9)	0.2142(4)	−0.1451(5)	0.0940	
O(4)	0.4691(8)	0.1591(4)	−0.4259(5)	0.0805	
O(5)	0.206(1)	−0.0412(5)	−0.4180(6)	0.1077	
O(6)	0.5978(8)	−0.0111(4)	−0.2134(6)	0.0911	
O(10)	0.3301(6)	0.0864(3)	−0.2820(4)	0.0574	
O(12)	0.2708(7)	0.1927(4)	−0.2490(5)	0.0798	
O(13)	0.1459(7)	0.0994(5)	−0.2453(5)	0.0848	
O(14)	0.2742(7)	0.1678(4)	−0.3806(4)	0.0741	
O(15)	0.1465(8)	0.0730(4)	−0.3773(5)	0.0833	
O(23)	0.3310(7)	0.1112(4)	−0.1509(4)	0.0793	
O(24)	0.4563(7)	0.1798(3)	−0.2864(4)	0.0665	
O(26)	0.5160(7)	0.1004(4)	−0.1864(4)	0.0680	
O(35)	0.2083(8)	−0.0080(4)	−0.2780(5)	0.0876	
O(36)	0.3931(8)	0.0059(4)	−0.1823(4)	0.0758	
O(45)	0.3334(7)	0.0614(4)	−0.4130(4)	0.0758	
O(46)	0.5181(7)	0.0740(4)	−0.3186(5)	0.0667	
O(56)	0.3944(8)	−0.0186(4)	−0.3136(5)	0.0782	
X(1)	0.0707(9)	0.1866(6)	−0.3494(6)	0.0871	
X(3)	0.198(1)	0.0137(6)	−0.1370(6)	0.0907	
C(1)*	0.019(3)	0.246(2)	−0.359(2)		0.141(5)
C(2)*	0.002(3)	0.278(2)	−0.427(2)		0.141(5)
C(3)*	−0.058(3)	0.333(2)	−0.436(2)		0.141(5)
C(4)*	−0.102(3)	0.353(2)	−0.385(2)		0.141(5)
C(5)*	−0.097(3)	0.326(2)	−0.323(2)		0.141(5)
C(6)*	−0.031(3)	0.269(2)	−0.305(2)		0.141(5)
C(7)**	0.117(4)	−0.003(3)	−0.096(3)		0.18(1)
C(8)**	0.074(5)	−0.061(3)	−0.109(2)		0.18(1)
C(9)**	−0.000(4)	−0.082(2)	−0.070(3)		0.18(1)
C(10)**	−0.031(5)	−0.045(3)	−0.019(3)		0.18(1)
C(11)**	0.013(6)	0.013(3)	−0.007(3)		0.18(1)
C(12)**	0.087(5)	0.034(2)	−0.045(3)		0.18(1)
N(32)	−0.2011(8)	0.0394(5)	−0.3691(5)	0.0683	
C(33)	−0.110(1)	−0.0064(7)	−0.3549(8)	0.0764	
C(34)	−0.094(1)	−0.0384(7)	−0.4203(8)	0.0861	
C(35)	−0.030(1)	−0.0955(8)	−0.3947(9)	0.0961	
C(36)	−0.017(1)	−0.1331(8)	−0.457(1)	0.1082	
C(37)	−0.218(1)	0.0608(7)	−0.2969(7)	0.0807	
C(38)	−0.116(1)	0.0907(8)	−0.2499(9)	0.0915	
C(39)	−0.151(2)	0.109(1)	−0.181(1)	0.1279	
C(40)	−0.205(3)	0.162(1)	−0.190(2)	0.1912	
C(41)	−0.309(1)	0.0132(6)	−0.4120(7)	0.0697	
C(42)	−0.340(1)	−0.0446(6)	−0.3826(8)	0.0847	
C(43)	−0.454(1)	−0.0646(7)	−0.4268(7)	0.0820	
C(44)	−0.486(2)	−0.1237(8)	−0.4005(9)	0.1101	
C(45)	−0.169(1)	0.0898(6)	−0.4117(7)	0.0744	
C(46)	−0.250(1)	0.1422(7)	−0.4224(9)	0.0911	
C(47)	−0.221(1)	0.1827(7)	−0.478(1)	0.1030	
C(48)	−0.291(2)	0.2380(8)	−0.487(1)	0.1297	
N(49)	0.426(1)	0.3411(5)	−0.4087(6)	0.0777	
C(50)	0.347(1)	0.3675(7)	−0.3693(8)	0.0898	
C(51)	0.296(2)	0.3201(8)	−0.330(1)	0.1119	
C(52)	0.213(3)	0.367(2)	−0.296(2)	0.1547	
C(53)	0.170(5)	0.329(2)	−0.263(2)	0.3039	
C(54)	0.465(1)	0.3944(6)	−0.4446(7)	0.0717	
C(55)	0.561(1)	0.3799(6)	−0.4778(8)	0.0841	

(continued)

Table 6 (*continued*)

Atom	*x/a*	*y/b*	*z/c*	U_{eq}	U_{iso}
C(56)	0.594(1)	0.4371(7)	−0.5082(8)	0.0920	
C(57)	0.692(1)	0.4273(9)	−0.5395(9)	0.1055	
C(58)	0.518(1)	0.3068(7)	−0.3579(8)	0.0887	
C(59)	0.583(2)	0.3469(8)	−0.298(1)	0.1155	
C(60)	0.664(2)	0.301(1)	−0.252(1)	0.1545	
C(61)	0.735(2)	0.333(1)	−0.196(1)	0.1735	
C(62)	0.370(1)	0.2949(6)	−0.4637(8)	0.0794	
C(63)	0.265(1)	0.3166(8)	−0.5159(9)	0.0982	
C(64)	0.222(2)	0.2621(9)	−0.566(1)	0.1213	
C(65)	0.115(2)	0.279(1)	−0.618(1)	0.1518	

X(1) = 0.58 N + 0.42 O.
X(3) = 0.34 N + 0.66 O.
* occ = 0.58.
**occ = 0.34.
[a]E.s.d.s in the least significant digits are given in parentheses.
[b]$U_{eq} = [U(11) \cdot U(22) \cdot U(33)]^{1/3}$.

average $(n\text{-}Bu_4N)_2[Mo_6O_{18.27}(NPh)_{0.83}]$ compound. Similarly, sample **3** would be a 79:8:13% mixture of $(n\text{-}Bu_4N)_2[Mo_6O_{18}(NPh)]$, $(n\text{-}Bu_4N)_2[Mo_6O_{19}]$ and $(n\text{-}Bu_4N)_2[Mo_6O_{17}(NPh)_2]$ and could be formulated as $(n\text{-}Bu_4N)_2[Mo_6O_{17.95}(NPh)_{1.05}]$. The situation is less clear for sample **1**, since its ^{95}Mo NMR spectrum displays at least a supplementary peak at 81 ppm in addition to those already discussed. This is tentatively attributed to a tris-imido species. Then, sample **1** would contain $[Mo_6O_{18}(NPh)]^{2-}$, $[Mo_6O_{17}(NPh)_2]^{2-}$ and $[Mo_6O_{16}(NPh)_3]^{2-}$ besides $[Mo_6O_{19}]^{2-}$.

3.2. Electrochemistry

The presence of several components in all samples is further reflected in their electrochemical behavior in acetonitrile. The polarograms and voltammograms of samples **2** and **3** have been recorded on the solutions used in NMR studies after being diluted 25 times. On the other hand, electrochemical studies of **1** were carried out on the recrystallized product while the NMR studies had dealt with a crude sample.

Polarograms at a rotating platinum electrode or at a DME show three reduction waves (Table 3). The first two waves at −0.37 and −0.56 V are well-defined, while the third one at about −0.73 V is often ill-defined and is more easily seen at a DME than at a platinum electrode. Considering the $E_{1/2}$ value of −0.37 V for the first reduction wave of an authentic sample of $(n\text{-}Bu_4N)_2[Mo_6O_{19}]$, the three waves can be respectively attributed to $[Mo_6O_{19}]^{2-}$, $[Mo_6O_{18}(NPh)]^{2-}$ and $[Mo_6O_{17}(NPh)_2]^{2-}$. The cathodic shift on going from the parent anion to the mono- and bis-imido derivatives is consistent with the trend in π-donor ability of the ligands, i.e. $O^{2-} < RN^{2-}$ [17a]. The relative proportions of the three components can be inferred from the wave heights (Table 8). Although there is a rather large uncertainty in the concentration of the bis-imido species, due to the poor definition of the third wave, the results are in satisfactory agreement with those calculated from NMR data, especially if the possibility of partial hydrolysis during the dilution is taken into account. According to electrochemical data, **1** would be a 60:20:20% mixture of $(n\text{-}Bu_4N)_2[Mo_6O_{18}(NPh)]$, $(n\text{-}Bu_4N)_2[Mo_6O_{19}]$ and $(n\text{-}Bu_4N)_2[Mo_6O_{17}(NPh)_2]$ and could be formulated as an averaged $(n\text{-}Bu_4N)_2[Mo_6O_{18.0}(NPh)_{1.0}]$ compound.

The voltammograms have been recorded at the same platinum electrode. Only in the case of sample **1**, the richest in the bis-imido species, was the third wave resolved; it was hardly visible for **3** and could not be seen for **2**. The three processes appear to be reversible according to the peak-to-peak separations (Table 3).

3.3. Vibrational spectroscopy

The IR spectra of samples **1**, **2** and **3** are quite similar to that of $(n\text{-}Bu_4N)_2[Mo_6O_{18}(NTol)]$ [1]. They differ from that of $(n\text{-}Bu_4N)_2[Mo_6O_{19}]$ only in the presence of weak bands characteristic of the phenyl group at 3060 and 1580 cm^{-1}, and bands at 1330 and 975 cm^{-1}. Most phenylimido complexes show a band in the 1310–1360 cm^{-1} region, which has been usually considered to be associated with the imido ligand on the basis of ^{15}N isotopic labeling studies; however, the actual origin of this band is still in dispute [17a].

Let us recall that the most characteristic Raman modes of $[Mo_6O_{19}]^{2-}$ are ν(M=O) at 986 (A_{1g}) and 958 (E_g) cm^{-1}, and ν(Mo–O_c) (vide infra) at 285 cm^{-1} [18]. The Raman spectra of samples **2** and **3** in acetonitrile display two lines at 986 and 284 cm^{-1}, which reveals the presence of $[Mo_6O_{19}]^{2-}$. According to line intensities, the relative amount of $[Mo_6O_{19}]^{2-}$ is greater in **2** than in **3**. In the 'high-frequency' region, the mono-

Table 7
Selected bond distances (Å) and angles (°) for $(n\text{-}Bu_4N)_2[Mo_6O_{17.84}(NPh)_{1.16}]$ (1) and $(n\text{-}Bu_4N)_2[Mo_6O_{18.08}(NPh)_{0.92}]$ (2)

	1	2
Mo(1)–O(10)	2.242(8)	2.265(8)
Mo(1)–O(12)	1.96(1)	1.97(1)
Mo(1)–O(13)	1.92(1)	1.929(9)
Mo(1)–O(14)	1.942(9)	1.921(8)
Mo(1)–O(15)	1.90(1)	1.889(9)
Mo(1)–X(1)	1.73(1)	1.68(1)
Mo(2)–O(2)	1.663(9)	1.685(9)
Mo(2)–O(10)	2.335(8)	2.335(8)
Mo(2)–O(12)	1.856(9)	1.879(9)
Mo(2)–O(23)	1.917(9)	1.908(9)
Mo(2)–O(24)	1.922(9)	1.941(8)
Mo(2)–O(26)	1.946(9)	1.922(9)
Mo(3)–O(10)	2.258(8)	2.291(8)
Mo(3)–O(13)	1.93(1)	1.91(1)
Mo(3)–O(23)	1.92(1)	1.902(9)
Mo(3)–O(35)	1.95(1)	1.935(9)
Mo(3)–O(36)	1.93(1)	1.927(9)
Mo(3)–X(3)	1.70(1)	1.68(1)
Mo(4)–O(4)	1.680(9)	1.677(8)
Mo(4)–O(10)	2.363(8)	2.332(8)
Mo(4)–O(14)	1.886(9)	1.908(9)
Mo(4)–O(24)	1.934(9)	1.921(8)
Mo(4)–O(45)	1.915(9)	1.903(8)
Mo(4)–O(46)	1.899(9)	1.897(8)
Mo(5)–O(5)	1.68(1)	1.67(1)
Mo(5)–O(10)	2.317(8)	2.305(8)
Mo(5)–O(15)	1.93(1)	1.94(1)
Mo(5)–O(35)	1.89(1)	1.923(9)
Mo(5)–O(45)	1.929(9)	1.914(8)
Mo(5)–O(56)	1.87(1)	1.89(1)
Mo(6)–O(6)	1.65(1)	1.668(9)
Mo(6)–O(10)	2.337(8)	2.328(8)
Mo(6)–O(26)	1.877(9)	1.890(8)
Mo(6)–O(36)	1.903(9)	1.896(8)
Mo(6)–O(46)	1.934(9)	1.950(8)
Mo(6)–O(56)	1.959(9)	1.952(9)
X(1)–C(1)	1.44(3)	1.48(4)
X(3)–C(7)	1.45(3)	1.49(4)
Mo(4)–O(10)–Mo(3)	178.8(4)	179.0(4)
Mo(5)–O(10)–Mo(2)	178.0(4)	179.1(4)
Mo(6)–O(10)–Mo(1)	178.3(4)	179.1(4)
C(1)–X(1)–Mo(1)	156.3(14)	151.8(17)
C(7)–X(3)–Mo(3)	154.4(18)	161.3(21)

X(1) = 0.76 N + 0.24 O for **1** and X(1) = 0.58 N + 0.42 O for **2**.
X(3) = 0.40 N + 0.60 O for **1** and X(3) = 0.34 N + 0.66 O for **2**.

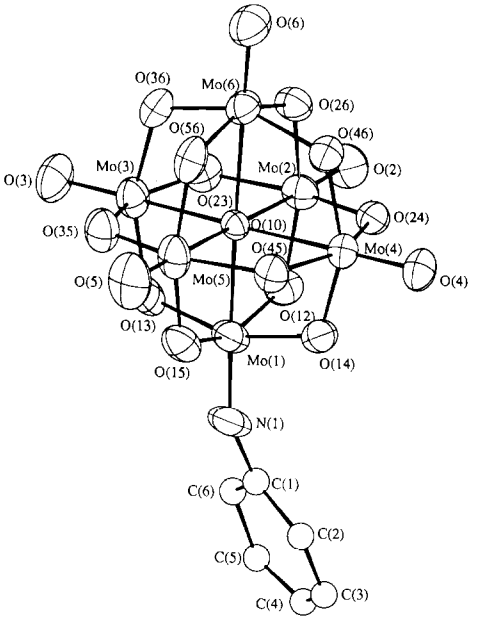

Fig. 4. Drawing [16] of $[Mo_6O_{18}(NPh)]^{2-}$.

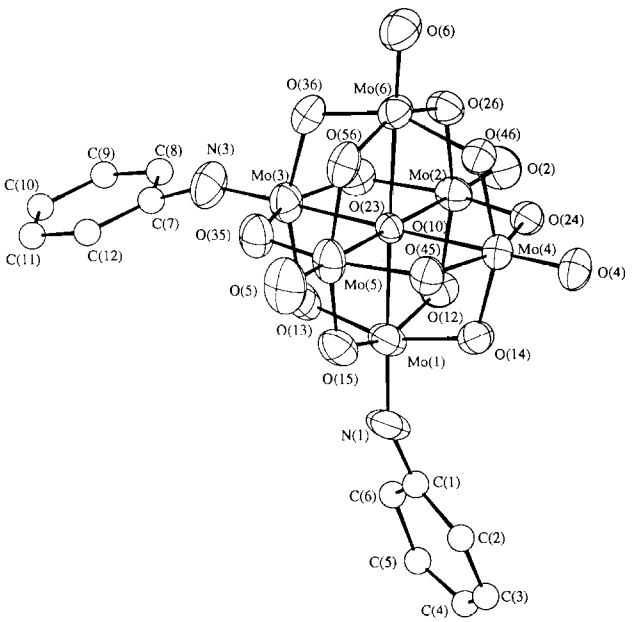

Fig. 5. Drawing [16] of *cis*-$[Mo_6O_{17}(NPh)_2]^{2-}$.

imido complex is characterized by two lines at 1004 (very strong) and 975 (medium) cm^{-1}; this could be interpreted either by a high-frequency shift by about 20 cm^{-1} of both ν(Mo=O)modes of the hexamolybdate anion or, more likely, by the result of the lowering of the anion symmetry from O_h to C_{4v}, which would allow the observation of separate Mo=O and Mo=N stretching modes. Such a splitting has been already observed in other substituted Lindqvist-type anions such as $[NbW_5O_{19}]^{3-}$ [19]. In the approximation of separate Mo=O and Mo=N vibrators, an internal coordinate analysis gives the following representation for the high-frequency modes:

$$\Gamma(Mo{=}O) = 2A_1(IR,R) + B_1(R) + E(IR,R)$$

$$\Gamma(Mo{=}N) = A_1(IR,R)$$

Under this assumption, the band at 975 cm^{-1} in the IR (solid state) and Raman (solution) spectra could be assigned to the A_1 ν(Mo=N) mode, which is in agreement with the proposition of Maatta and coworkers concerning the attribution of the band at 980 cm^{-1} for the mono-tolylimido derivative [1]. The other intense Raman line at 1004 cm^{-1} would arise from

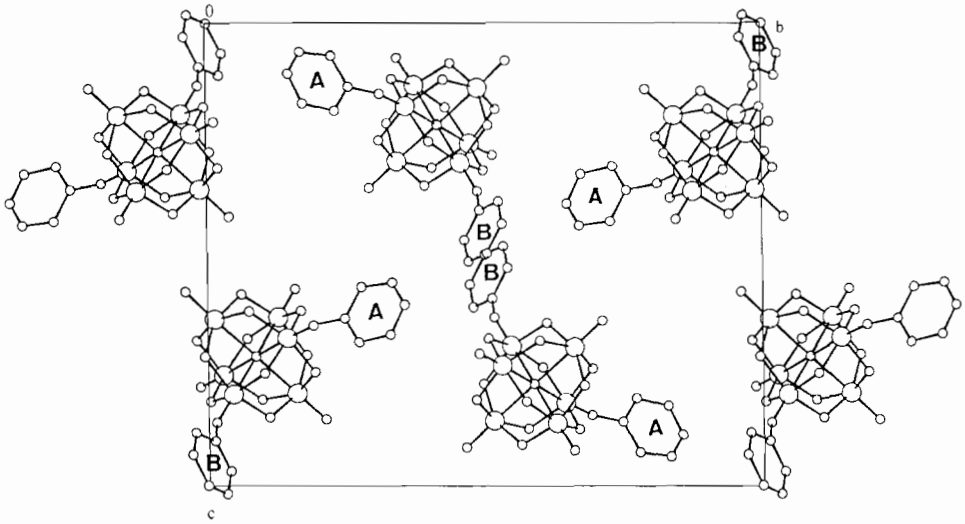

Fig. 6. View [16] of the packing in **1**.

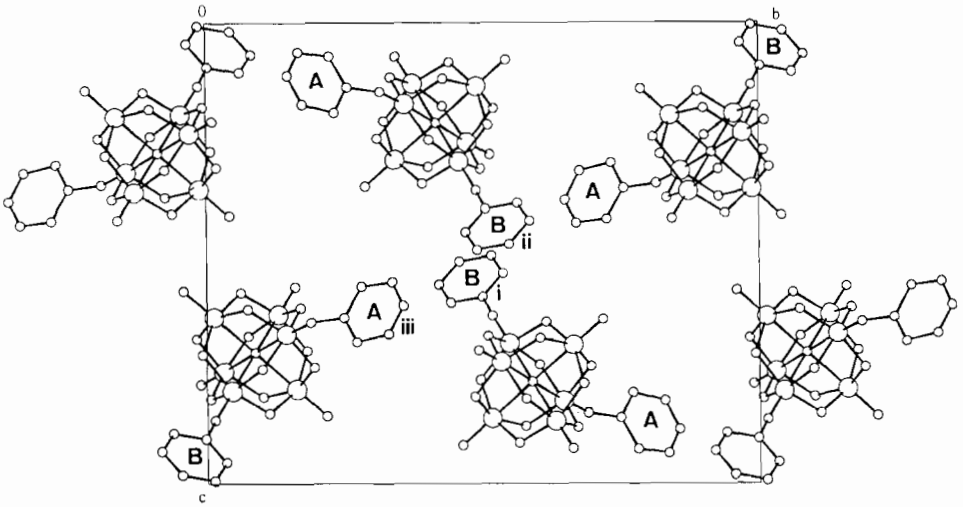

Fig. 7. View [16] of the packing in **2**.

Table 8
Relative proportions of the molybdo species determined by different physicochemical methods

Method	Sample **1**						Sample **2**						Sample 3					
	m/h	m/b	m	h	b	*x*	m/h	m/b	m	h	b	*x*	m/h	m/b	m	h	b	*x*
^{95}Mo NMR		1.5[a]					3[b]	12[a]	71	23	6	0.83	10[b]	6[a]	79	8	13	1.05
^{14}N NMR		1.5[c]						12[c]						6[c]				
Electrochemistry	3	3	60	20	20	1	2						6	9	78	13	9	0.96
Raman spectroscopy[d]							3	15	71	24	5	0.81	7	6	76	11	13	1.02

m = mono-imido; b = bis-imido; h = hexamolybdate m + h + b = 100; *x* = mean degree of substitution.

[a]From the integration of the *Mo*=N resonances.

[b]Taking into account a contribution from the monoimido anion to the 125 ppm hexamolybdate resonance.

[c]From the integration of the *N*=Mo resonances. Concentration of $[Mo_6O_{19}]^{2-}$ only indirectly by difference from the integration of the resonance of the n-Bu_4N^+ cation.

[d]Assuming that the probability of the Raman transition 'ν_s(Mö–O_c)' is the same for all species.

the A_1 ν_s(Mo=O) mode while the band at 956 cm^{-1}, which appears in both IR and Raman spectra, would be due to the ν_{as}(Mo=O) mode. As usual in the vibrational spectra of polyoxo anions, the symmetry-allowed modes are not all observed, because of either too low intensity or/and accidental degeneracy.

The low-frequency region of the Raman spectrum is even more informative as lines relative to the three species appear at well separated wavenumbers, 285, 256 and 240 cm^{-1}, for $[Mo_6O_{19}]^{2-}$, $[Mo_6O_{18}(NPh)]^{2-}$ and $[Mo_6O_{17}(NPh)_2]^{2-}$, respectively (Fig. 2). As shown by a normal coordinate analysis on the hexamolybdate anion, this mode essentially involves Mo–O_b and MoO_c stretches; it can be described as a 'breathing' of the whole cage around the central oxygen O_c and will be shortly noted as ν_s(Mo–O_c) [18,20]. Its frequency was shown to be very sensitive to metal substitution in the hexametalate framework: in particular, a 17 cm^{-1} low-frequency shift is observed on going from $[MoW_5O_{19}]^{2-}$ to $[W_6O_{19}]^{2-}$ [20,21]. The replacement of one terminal oxo ligand by a phenylimido ligand appears to produce a similar effect to that of the replacement of one Mo by W in the hexametalate.

Assuming in a first approximation that the Raman transition probability for this mode is the same for $[Mo_6O_{19}]^{2-}$, $[Mo_6O_{18}(NPh)]^{2-}$ and $[Mo_6O_{17}(NPh)_2]^{2-}$, we can obtain an estimation of the concentrations of these species in the two samples; the results agree with other measurements (Table 8).

3.4. Electronic spectroscopy

The electronic spectra of **1–3** in acetonitrile solution show three bands at 342 (log ϵ ~4.3), 250 (log ϵ ~4.4) and 225 (log ϵ ~4.5) nm. These features are quite similar to those of $[Mo_6O_{19}]^{2-}$ which displays three bands at 325 (log ϵ ~3.8), 260 (log ϵ ~4.1) and 225 (log ϵ ~4.3) nm. The lowest-energy transition in $[Mo_6O_{19}]^{2-}$ was assigned to a charge-transfer transition from the oxygen π-type non-bonding HOMO to the molybdenum π-type LUMO [22]. The bathochromic shift on going from $[Mo_6O_{19}]^{2-}$ to phenylimido derivatives is consistent with the trend in π-donor ability of the ligands [17a].

3.5. Solid-state studies

The sets of cell parameters of samples **1**, **2** and **3** (Table 4) display only small but significant variations in the values of b and β, and are similar to that of (n-$Bu_4N)_2[Mo_6O_{19}]$ [23]. From the X-ray studies, the composition of samples **1** and **2** was determined to be (n-$Bu_4N)_2[Mo_6O_{19-x}(NPh)_x]$ with $x = 1.16$ and 0.92, respectively. In the case of **3**, three different crystals were tested: all display the same unit cell parameters. Although the X-ray crystal structure of **3** was not determined, solution studies indicate that x should lie between the values for **1** and **2**, which is consistent with electrochemical results. Thus, it is tempting (i) to consider that the composition of a given crystal is representative of the composition of the whole sample and (ii) to correlate the value of x with that of β. Indeed, the β value increases as the mean degree of substitution decreases.

The unit cells of both **1** and **2** were found to contain four hexametalate anions and eight tetrabutylammonium cations. It is clear that both samples contain a mixture of at least two (possibly three) different anions. Even when x is greater than 1, e.g. **1**, it cannot be excluded that $[Mo_6O_{19}]^{2-}$ is present in the crystal, although we were unable to provide a direct confirmation of this. Although the x range has not yet been determined, samples **1**, **2** and **3** can be viewed as solid solutions of (n-$Bu_4N)_2[Mo_6O_{18}(NPh)]$, (n-$Bu_4N)_2$[*cis*-$Mo_6O_{17}(NPh)_2$] and, eventually, (n-$Bu_4N)_2[Mo_6O_{19}]$.

The disorder precludes a detailed analysis of the effect of the substitution of a phenylimido ligand for an oxo ligand. Nevertheless, some general trends can be drawn. The structural parameters of the averaged substituted anions are not very different from those of $[Mo_6O_{18}(NTol)]^{2-}$ [1]. Although multiple bond lengths in general vary in the order oxo < imido, which correlates with the covalent radii of the ligating atoms [17a], the Mo–N bond lengths in arylimido derivatives of $[Mo_6O_{19}]^{2-}$ are hardly significantly longer than the Mo–O_t bond lengths. This was already noticed for the tolylimido derivative [1]. However, it must be recalled that each Mo–X bond in **1** and **2** has some Mo–O_t character, so the apparent bond length should lie between those of true Mo–N and true Mo–O bonds. Although the estimated standard deviations are rather large, it is worth pointing out that the longer distance is observed for Mo(1)–X(1) in **1**, i.e. the bond with the highest Mo–N character. The Mo–N bond lengths in imido derivatives of $[Mo_6O_{19}]^{2-}$ are consistent with linear imido ligands although the Mo–X–C angles depart from linearity more than expected [17b]. The lowest value of 151.8(17)° observed for Mo(3)–X(3)–C(7) in **2** is still clearly larger than the value of 139.4(4)° observed for the bent imido ligand in $[Mo(NPh)_2(S_2CNEt_2)_2]$ [24].

The distortion of the hexanuclear core of molybdenum atoms with respect to $[Mo_6O_{19}]^{2-}$ appears to be rather small in comparison with $[Mo_5O_{18}\{Ti(Cp)\}]^{3-}$ [25], $[Mo_5O_{18}\{Mo(NNAr)\}]^{3-}$ [3] and $[Mo_5O_{18}\{Mo(Cp^*)\}]^{-}$ [5]. Nevertheless, Mo(1)–O(10) and Mo(3)–O(10) are significantly shorter than the average of other Mo–O(10) distances, which could indicate that the *trans* influence of the phenylimido ligand is weaker than that of the oxo ligand. Inspection of bond lengths in the Mo(1)–O(12)–Mo(2)–O(26)–Mo(6)–O(56)–Mo(5)–

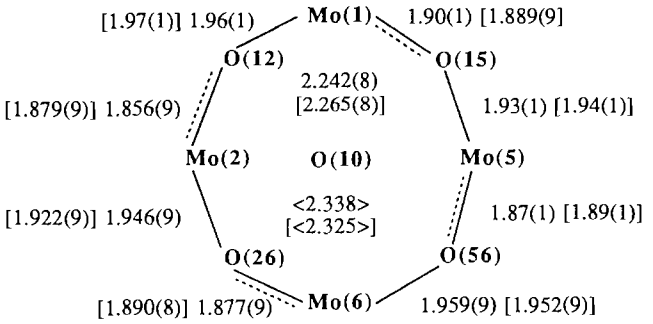

Scheme 1.

O(15) ring reveals a pattern of bond length alternation (Scheme 1).This is reminiscent of the Mo–O_b bond length alternation in the three sets of $Mo_4(O_b)_4$ rings present in the centrosymmetric $[Mo_6O_{19}]^{2-}$ anion [26], which has been explained on the basis of an off-center displacement of metal atoms [25]. On the other hand, it differs from the pattern observed in other derivatives of $[Mo_6O_{19}]^{2-}$, where *both* Mo–O_b involving the modified metal center are lengthened. Although there are no significant differences between **1** and **2**, the Mo–O(10) distances involving the molybdenum atoms bearing an imido ligand seem to correlate with the occupancy factor of the imido ligand, i.e. the higher the Mo–N character, the lower the Mo–O(10) distance. Thus, it cannot be excluded that the specific pattern observed in **1** and **2** merely reflects an averaged geometry. Indeed, it has been reported that the tolylimido derivative displays the expected pattern of Mo–O_b bond lengths [1].

4. Conclusions

Both $(n\text{-}Bu_4N)_2[Mo_6O_{18}(NPh)]$ and $(n\text{-}Bu_4N)_2[Mo_6O_{17}(NPh)_2]$ are formed in the reaction of $(n\text{-}Bu_4N)_2[Mo_6O_{19}]$ with either 1 or 2 equiv. of $Ph_3P{=}NPh$ in pyridine or acetonitrile. There is also some ^{95}Mo NMR evidence for the formation of the tris-imido derivative. The formation of the bis-imido derivative even when only 1 equiv. of $Ph_3P{=}NPh$ is used means either $[Mo_6O_{18}(NPh)]^{2-}$ is less stable than $[Mo_6O_{17}(NPh)_2]^{2-}$, which seems rather unlikely, or that the former is more reactive than $[Mo_6O_{19}]^{2-}$ and reacts competitively with it. ^{95}Mo and ^{14}N NMR, Raman and electrochemical solution studies led to the conclusion that all samples contain $(n\text{-}Bu_4N)_2[Mo_6O_{19}]$ together with $(n\text{-}Bu_4N)_2[Mo_6O_{18}(NPh)]$ and $(n\text{-}Bu_4N)_2[Mo_6O_{17}(NPh)_2]$. Contamination with $[Mo_6O_{19}]^{2-}$ could arise from partial hydrolysis of the imido derivatives either during initial workup or during the dissolution and dilution processes. It was found that the addition of 3 or 4 drops of water in the electrochemical cell had no immediate effect on the polarogram although an increase in the proportion of $[Mo_6O_{19}]^{2-}$ was observed a few days later. This suggests that the importance of hydrolysis should not be overestimated. Nevertheless, it could account for some difference between the compositions deduced from solid-state and solution studies. This would be especially true for sample **1**, where the value obtained from the X-ray study is to be compared with that obtained from electrochemical data.

Further studies will focus on the separation and on the characterization of the individual imido derivatives by use of suitable cations.

5. Supplementary material

X-ray diffraction data are available from the authors on request.

References

[1] Y.H. Du, A.L. Rheingold and E.A. Maatta, *J. Am. Chem. Soc., 114* (1992) 345.
[2] H. Kang and J. Zubieta, *J. Chem. Soc., Chem. Commun.,* (1988) 1192.
[3] (a) T.-C. Hsieh and J. Zubieta, *Polyhedron, 5* (1986) 1655; (b) S. Bank, S. Liu, S.-N. Shaikh, X. Sun, J. Zubieta and P.D. Ellis, *Inorg. Chem., 27* (1988) 3535.
[4] (a) P. Gouzerh, Y. Jeannin, A. Proust and F. Robert, *Angew. Chem., Int. Ed. Engl., 28* (1989) 1363; (b) A Proust, R. Thouvenot, F. Robert and P. Gouzerh, *Inorg. Chem., 32* (1993) 5299.
[5] F. Bottomley and J. Chen, *Organometallics, 11* (1992) 3404.
[6] J.R. Harper and A.L. Rheingold, *J. Am. Chem. Soc., 112* (1990) 4037.
[7] L. Barcza and M.T. Pope, *J. Phys. Chem., 79* (1975) 92.
[8] S. Liu, S.-N. Shaikh and J. Zubieta, *Inorg. Chem., 28* (1989) 723.
[9] A. Proust, P. Gouzerh and F. Robert, *J. Chem. Soc., Dalton Trans.,* (1994) 819.
[10] N.H. Hur, W.G. Klemperer and R.-C. Wang, *Inorg. Synth., 27* (1990) 77.
[11] (a) M. Witanowski, L. Stefaniak and G.A. Webb, in G.A. Webb (ed.), *Nitrogen Spectroscopy in Annual Report on NMR Spectroscopy,* Vol. 11B, Academic Press, London, 1981, p. 304; (b) M. Witanowski, L. Stefaniak, M. Kamienski, S. Biernat and G.A. Webb, *J. Magn. Reson., 43* (1981) 456.
[12] D.J. Watkin, J.R. Carruthers and P.W. Betteridge, *Crystals User Guide,* Chemical Crystallography Laboratory, University of Oxford, Oxford, UK, 1992.
[13] G.M. Sheldrick, *SHELXS 86*, a program for crystal structure determination, Göttingen, Germany, 1986.
[14] N. Walker and D. Stuart, *Acta Crystallogr., Sect. A, 39* (1983) 158.
[15] *International Table for X-Ray Crystallography,* Vol. IV, Kynoch, Birmingham, UK, 1974, pp. 149–150.
[16] L.J. Pearce and D.J. Watkin, *CAMERON,* Chemical Crystallography Laboratory, University of Oxford, Oxford, UK, 1992.
[17] (a) W. Nugent and J.E. Mayer, *Metal–Ligand Multiple Bonds,* Wiley, New York, 1988, Ch. 4, p. 112; (b) Ch. 5, p. 145.
[18] C. Rocchiccioli-Deltcheff, R. Thouvenot and M. Fouassier, *Inorg. Chem., 21* (1982) 30.

[19] C. Rocchiccioli-Deltcheff, R. Thouvenot and M. Dabbabi, *Spectrochim. Acta, Part A, 33* (1977) 143.
[20] C. Rocchiccioli-Deltcheff, M. Fournier, R. Franck and R. Thouvenot, *Spectrosc. Lett., 19* (1986) 765.
[21] M. Fournier and R. Thouvenot, manuscript in preparation.
[22] (a) M. Fournier, C. Louis, M. Che, P. Chaquin and D. Masure, *J. Catal., 119* (1989) 400; (b) D. Masure, P. Chaquin, C. Louis, M. Che and M. Fournier, *J. Catal., 119* (1989) 415.
[23] P. Dahlstrom, J. Zubieta, B. Neaves and J.R. Dilworth, *Cryst. Struct. Commun., 11* (1982) 463.
[24] B.L. Haymore, E.A. Maatta and R.A.D. Wentworth, *J. Am. Chem. Soc., 101* (1979) 2063.
[25] T.M. Che, V.W. Day, L.C. Francesconi, M.F. Fredrich and W.G. Klemperer, *Inorg. Chem., 24* (1985) 4055.
[26] H.R. Allcock, E.C. Bissell and E.T. Shawl, *Inorg. Chem., 12* (1973) 2963.

Note added in proof

The butylimido derivative of $[Mo_6O_{19}]^{2-}$ has been recently mentioned: R.J. Errington, C. Lax, D.G. Richards, W. Clegg and K.A. Fraser, in M.T. Pope and A. Müller (eds.), *Polyoxometalates: From Platonic Solids to Anti-Retroviral Activity*, Kluwer, Dordrecht, Netherlands, 1994, p. 105. Poly-imido derivatives have also been reported: J.B. Strong, R. Ostrander, A.L. Rheingold and E.A. Maatta, *J. Am. Chem. Soc., 116* (1994) 3601.